Aalto University

OPEN ACCESS

This is an electronic reprint of the original article.
This reprint may differ from the original in pagination and typographic detail.

Wang, J.; Pesquera, D.; Mansell, R.; Van Dijken, S.; Cowburn, R. P.; Ghidini, M.; Mathur, N. D.

Giant non-volatile magnetoelectric effects via growth anisotropy in $Co_{40}Fe_{40}B_{20}$ films on PMN-PT substrates

Published in:
Applied Physics Letters

DOI:
10.1063/1.5078787

Published: 04/03/2019

Document Version
Publisher's PDF, also known as Version of record

Please cite the original version:
Wang, J., Pesquera, D., Mansell, R., Van Dijken, S., Cowburn, R. P., Ghidini, M., & Mathur, N. D. (2019). Giant non-volatile magnetoelectric effects via growth anisotropy in $Co_{40}Fe_{40}B_{20}$ films on PMN-PT substrates. *Applied Physics Letters*, *114*(9), 1-4. Article 092401. https://doi.org/10.1063/1.5078787

This material is protected by copyright and other intellectual property rights, and duplication or sale of all or part of any of the repository collections is not permitted, except that material may be duplicated by you for your research use or educational purposes in electronic or print form. You must obtain permission for any other use. Electronic or print copies may not be offered, whether for sale or otherwise to anyone who is not an authorised user.

Applied Physics Letters

Giant non-volatile magnetoelectric effects via growth anisotropy in $Co_{40}Fe_{40}B_{20}$ films on PMN-PT substrates

Cite as: Appl. Phys. Lett. **114**, 092401 (2019); https://doi.org/10.1063/1.5078787
Submitted: 29 October 2018 . Accepted: 13 February 2019 . Published Online: 05 March 2019

J. Wang, D. Pesquera, R. Mansell, S. van Dijken, R. P. Cowburn, M. Ghidini, and N. D. Mathur

View Online
Export Citation
CrossMark

ARTICLES YOU MAY BE INTERESTED IN

Spin-orbit torque-induced magnetization switching in epitaxial Au/Fe_4N bilayer films
Applied Physics Letters **114**, 092402 (2019); https://doi.org/10.1063/1.5078395

Magnetic-field control of ionic bonds on ferroelectric surfaces
Applied Physics Letters **114**, 091601 (2019); https://doi.org/10.1063/1.5061718

Spin valve effect induced by spin-orbit torque switching
Applied Physics Letters **114**, 092404 (2019); https://doi.org/10.1063/1.5086775

AIP Publishing

© 2019 Author(s).

Applied Physics Letters ARTICLE scitation.org/journal/apl

Giant non-volatile magnetoelectric effects via growth anisotropy in $Co_{40}Fe_{40}B_{20}$ films on PMN-PT substrates

Cite as: Appl. Phys. Lett. **114**, 092401 (2019); doi: 10.1063/1.5078787
Submitted: 29 October 2018 · Accepted: 13 February 2019 ·
Published Online: 5 March 2019

J. Wang,[1,2] D. Pesquera,[2] R. Mansell,[3,4] S. van Dijken,[4] R. P. Cowburn,[3] M. Ghidini,[5,6,2,a)] and N. D. Mathur[2,b)]

AFFILIATIONS

[1]State Key Laboratory of Mechanics and Control of Mechanical Structures, College of Aerospace Engineering, Nanjing University of Aeronautics and Astronautics, Nanjing 210016, People's Republic of China
[2]Department of Materials Science, University of Cambridge, Cambridge CB3 0FS, United Kingdom
[3]Cavendish Laboratory, University of Cambridge, Cambridge CB3 0HE, United Kingdom
[4]NanoSpin, Department of Applied Physics, Aalto University School of Science, P.O. Box 15100, FI-00076 Aalto, Finland
[5]Department of Mathematics, Physics and Computer Science, University of Parma, 43124 Parma, Italy
[6]Diamond Light Source, Chilton, Didcot, Oxfordshire OX11 0DE, United Kingdom

[a)]massimo.ghidini@unipr.it
[b)]ndm12@cam.ac.uk

ABSTRACT

Uniaxial magnetic anisotropy was imposed on a CoFeB film by applying an in-plane magnetic field during growth. Electrically driven strain from a ferroelectric $0.68Pb(Mg_{1/3}Nb_{2/3})O_3$-$0.32PbTiO_3$ (011) substrate resulted in giant magnetoelectric effects, whose coupling constant peaked at a record value of $\sim 8.0 \times 10^{-6}$ s m^{-1}. These large magnetoelectric effects arose due to non-volatile 90° rotations of the magnetic easy axis, reflecting a competition between the fixed growth anisotropy and the voltage-controlled magnetoelastic anisotropy. In contrast to previous work, our non-volatile rotations did not require the assistance of an applied magnetic field or the setting of an in-plane substrate polarization prior to deposition.

Published under license by AIP Publishing. https://doi.org/10.1063/1.5078787

The renaissance of magnetoelectric materials and devices[1–4] is driven by the technological goal of developing magnetoelectric random access memories (MERAMs),[5,6] in which converse magnetoelectric effects (CMEs) permit data to be written electrically with a voltage rather than magnetically with a current, thus consuming less power. It is therefore necessary to identify systems in which a large magnetization undergoes electrically driven switching that is repeatable and non-volatile, at room temperature, with no assistance from a variable magnetic field.

CMEs have been demonstrated in a range of systems, namely, multiferroic materials,[1–3,7,8] ferromagnetic semiconductors,[9–12] ultra-thin ferromagnetic films addressed via back gates,[13,14] and ferromagnetic films addressed via materials that are ferroelectric,[15–26] antiferromagnetic,[27] or both.[28,29] Large voltage-driven switches of net magnetization have only been achieved in the latter systems,[15–29] for example, via strain from ferroelectric substrates of $BaTiO_3$ (BTO)[30,31] and $(1–x)Pb(Mg_{1/3}Nb_{2/3})O_3–xPbTiO_3$ (PMN-PT, with $x \sim 0.3$).[24–26] However, the vast majority of strain-mediated CMEs are volatile because the ferroelectric substrates show voltage-strain "butterfly" characteristics that are single-valued at zero electric field.[15,30–35] Non-volatile CMEs include 90° rotations[24–26] and reversals[28,29] but suffer the need for magnetic-field assistance,[26,28] the need for setting an in-plane polarization before deposition,[24,25] or inhomogeneity.[29]

Here, we use voltage-driven anisotropic strain from ferroelectric substrates of PMN-PT (011) to control the magnetization in ferromagnetic films of $Co_{40}Fe_{40}B_{20}$ (CFB). Voltage-driven 90° rotations of the easy-axis were achieved in a repeatable and non-volatile manner due to the competition between the voltage-controlled magnetoelastic anisotropy arising from the substrate and a fixed uniaxial magnetic anisotropy that we imposed by applying a magnetic field during film growth. Our non-volatile CME displays a record magnetoelectric coupling coefficient of $\sim 8.0 \times 10^{-6}$ s m^{-1} and moreover represents a qualitative improvement with respect to all but one[29] previously reported[24–26,28] non-volatile CMEs for two reasons. First, we did not require the assistance of a magnetic field.[26,28] Second, we prepared the substrate for deposition by applying a large poling field rather than setting the polarization in-plane using a carefully tuned field whose magnitude is substrate dependent.[24,25]

We used a 0.3 mm-thick substrate of rhombohedral PMN-PT $(011)_{pc}$ from Atom Optics (pc denotes pseudocubic). X-ray diffraction with a four-circle high-resolution Panalytical Empyrean vertical diffractometer was used to confirm that the long substrate edges were aligned with $x \,||\, [100]_{pc}$ and $y \,||\, [0\bar{1}1]_{pc}$ [Figs. 1(a) and 1(b)]. In order to avoid virgin CMEs, the substrate was poled along $-z$ by applying an electric field of $E = -1\,\mathrm{MV\ m^{-1}}$ between a back electrode of sputter-deposited Pt and a temporary top electrode of silver paste.

After dissolving our temporary electrode, we applied ~30 Oe in-plane along $x \,||\, [100]_{pc}$ [Figs. 1(a) and 1(b)], set a base pressure of 6×10^{-8} mbar, and used magnetron sputtering to deposit first the 50 nm CFB film and then a 5 nm Pt cap to prevent oxidation (both films were grown at 50 W in 2.7×10^{-3} mbar Ar). X-ray diffraction revealed the CFB film to be amorphous, and the CFB/Pt bilayer served as a grounded top electrode.

After cleaving the sample into two, we used one part for all magnetic measurements and the other part for all strain measurements. CMEs were measured with a Princeton Measurements Corporation vibrating sample magnetometer, using a bespoke probe with electrical wiring that was constructed in-house.[16] Strain measurements were performed by gluing a biaxial strain gauge (KFG-1–120-D16-16L1M3S, KYOWA) to the CFB film.

The magnetic field that was applied along x during growth caused the CFB film to display uniaxial magnetic anisotropy, as seen via magnetic hysteresis loops [Fig. 1(c)] and a polar plot of squareness [Fig. 1(d)] that was constructed from 18 such loops. For our poled sample, the magnetic easy axis (EA) with $M_r/M_s \sim 1$ was parallel to x, and the hard axis (HA) with $M_r/M_s \sim 0.07$ was parallel to y (where M_r denotes the remanent magnetization and M_s denotes the saturation magnetization).

Bipolar measurements of the piezoelectric effect in our PMN-PT substrate were performed with the CFB/Pt bilayer present as the top electrode. The primarily compressive x-axis strain $\varepsilon_x(E)$ [Fig. 2(a)] took the form of a weakly hysteretic "butterfly" that was single-valued at $E \sim 0$ (rather than $E = 0$, evidencing a small imprint). By contrast, the primarily tensile y-axis strain $\varepsilon_y(E)$ [Fig. 2(b)] displayed a pronounced asymmetry that rendered it hysteretic and thus bistable at $E = 0$. It follows that the resulting anisotropic strain $\varepsilon_y - \varepsilon_x$ [Fig. 2(c)] was also bistable at $E = 0$, and we will see later that the two zero-field values of $\varepsilon_y - \varepsilon_x$ lie above and below the critical strain ε_{cr} that determines the EA orientation.

Zero-magnetic-field CME measurements of $M_x(E)$ [Fig. 3(a)] and $M_y(E)$ [Fig. 3(b)] reveal two states of magnetization at $E = 0$, consistent with an electrically controlled strain that rotates the EA between y (green data) and x (red or blue data). [Note that all values of $M_x(E)$ are relatively small because the pre-measurement magnetic saturation was performed when the x axis was electrically set to be magnetically hard.] As expected, the CME coupling coefficients $\alpha_x = \mu_0 \mathrm{d}M_x/\mathrm{d}E$ [Fig. 3(c)] and $\alpha_y = \mu_0 \mathrm{d}M_y/\mathrm{d}E$ [Fig. 3(d)] were the largest near the coercive fields of the ferroelectric substrate.

Magnetic hysteresis loops [Figs. 4(a)–4(c)] and polar plots [Figs. 4(d)–4(f)] confirm that the EA and HA underwent non-volatile interconversions when we applied and removed saturating electric fields of fixed magnitude (0.67 $\mathrm{MV\ m^{-1}}$) and alternate sign. Specifically, the

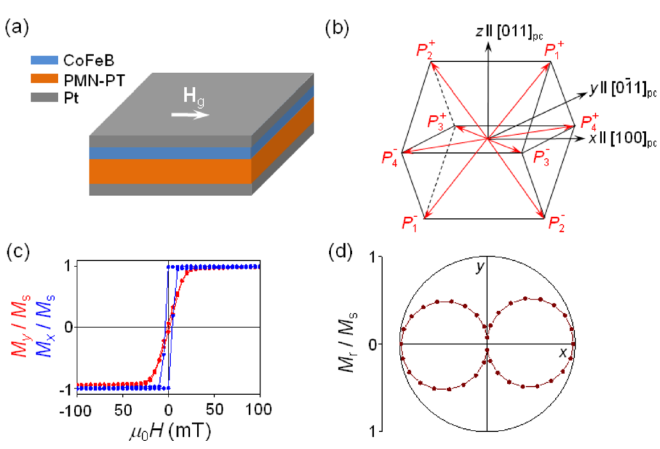

FIG. 1. Sample structure and uniaxial magnetic anisotropy. (a) Sample schematic, not to scale. Magnetic field $\mathbf{H}_g$ was applied along x during film growth. (b) The pseudocubic (pc) unit cell of the PMN-PT substrate, whose edges were collinear with the Cartesian directions denoted by black arrows, such that the $(011)_{pc}$ surface lay in the x-y plane. Red arrows denote permitted $\langle 111 \rangle_{pc}$ directions of local polarization. (c) Reduced components of magnetization M_x/M_s (blue) and M_y/M_s (red) versus collinear magnetic field H, prior to the application of any electric field. (d) Polar plot of loop squareness M_r/M_s derived from plots such as those shown in (c). Here, M_r denotes the remanent magnetization and M_s denotes the saturation magnetization.

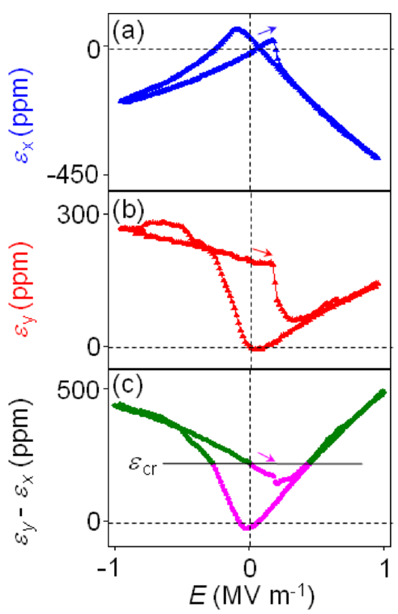

FIG. 2. Piezoelectric response of the PMN-PT substrate. In-plane strains (a) ε_x and (b) ε_y, and hence (c) anisotropic strain $\varepsilon_y - \varepsilon_x$, versus electric field E. When $\varepsilon_y - \varepsilon_x$ was larger (smaller) than the critical strain of $\varepsilon_{cr} \sim 220$ ppm, as shown by colouring data green (pink), the magnetic easy axis of the CFB film lay along y (along x). The CFB film served as the top electrode.

Published under license by AIP Publishing

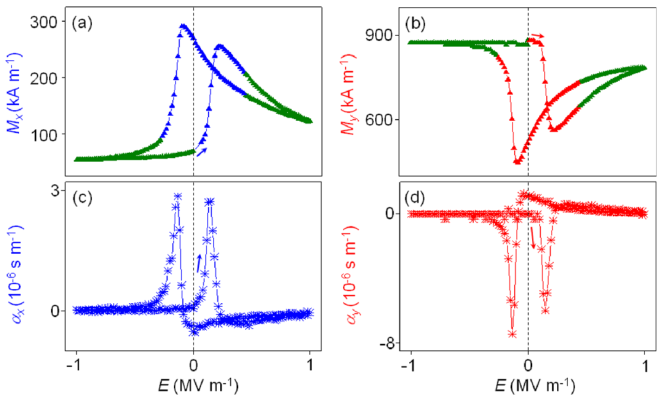

FIG. 3. Magnetoelectric effects. Variation of (a) M_x and (b) M_y with the electric field E, after electrically setting the easy axis parallel to y, applying and removing 500 mT along the measurement direction, and sweeping the electric field through one complete cycle prior to data collection. The corresponding magnetoelectric coupling coefficients are (c) $\alpha_x = \mu_0 \mathrm{d}M_x/\mathrm{d}E$ and (d) $\alpha_y = \mu_0 \mathrm{d}M_y/\mathrm{d}E$. Green data identify fields for which the EA was understood to lie along y [cf. Fig. 2(c)].

application and removal of a large negative field aligned the EA along y, while the application and removal of a large positive field aligned the EA along x. This switching is consistent with the non-volatile CMEs that we observed when sweeping an electric field [Figs. 3(a) and 3(b)], and it permits electric field pulses of alternate sign [Fig. 5(a)] to switch a large net magnetization as measured along both the y axis [Fig. 5(b)] and the x axis [Fig. 5(c)]. This electrically driven switching is non-volatile, repeatable, and did not require the assistance of a magnetic field[26,28] or the setting of an in-plane substrate polarization.[24,25] [Again, all values of $M_x(E)$ are relatively small because the pre-measurement magnetic saturation was performed when the x axis was electrically set to be magnetically hard.]

Our non-volatile CMEs (Figs. 3–5) result from electrically driven 90° rotations of the EA (Fig. 4), which may be understood in terms of

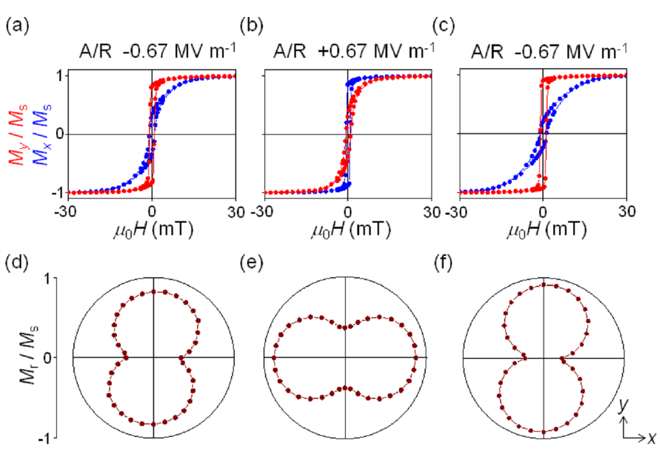

FIG. 4. Electrically driven changes of loop squareness. (a)–(c) Reduced components of magnetization M_x/M_s (blue) and M_y/M_s (red) versus collinear magnetic field H, after applying and removing (a) -0.67 MV m^{-1}, (b) $+0.67$ MV m^{-1}, and (c) -0.67 MV m^{-1}. (d)–(f) The corresponding polar plots of loop squareness M_r/M_s derived from plots such as those shown in (a)–(c).

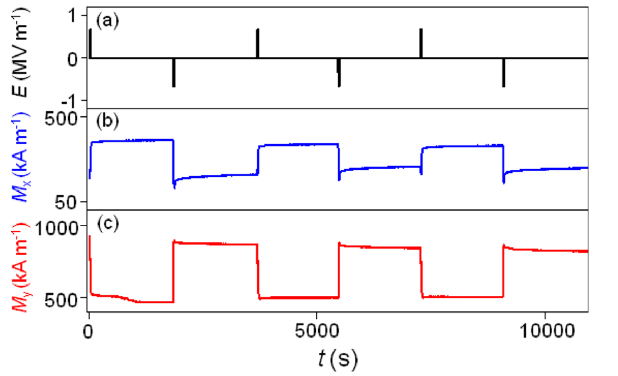

FIG. 5. Magnetoelectric switching. (a) Pulses of electric field E versus time t, and the resulting changes in (b) M_x and (c) M_y, after electrically setting the easy axis parallel to y, and applying and removing 500 mT along the measurement direction. The large interval between switching events confirms good stability.

a competition between the growth-anisotropy energy $K_g \sin^2\theta$ and the magnetoelastic energy $\frac{3}{2}E_Y\lambda(\varepsilon_y - \varepsilon_x)\cos^2\theta = K_u \cos^2\theta$ arising from the anisotropic strain $\varepsilon_y - \varepsilon_x$ [Fig. 2(c)]. Here, $K_g > 0$ is the growth-anisotropy constant, K_u is the magnetoelastic energy constant, E_Y is the Young's modulus of the CFB film, $\lambda > 0$ is the magnetostriction of the CFB film, and θ is the angle that the in-plane CFB magnetization makes with the x-axis.

The resulting total energy density $(K_u - K_g)\cos^2\theta$ implies an EA along y for $K_u > K_g$ and an EA along x for $K_u < K_g$. Therefore, the EA is expected to switch from x to y when $\varepsilon_y - \varepsilon_x$ exceeds a critical strain of $\varepsilon_{cr} = 2K_g/3\lambda E_Y \sim 245$ ppm, where $K_g = \frac{1}{2}\mu_0 M_s H_k = 6$ kJ m^{-3} from the HA measurement of magnetisation [Fig. 1(c) with anisotropy field $\mu_0 H_k = 15$ mT and $M_s = 0.8$ MA m^{-1}], $\lambda = 75$ ppm for a similar material,[36] and $E_Y = 216$ GPa from Ref. 37. Our measurements of anisotropic strain imply that a similar value of $\varepsilon_{cr} \sim 220$ ppm would be just small enough to permit the two EA orientations at $E = 0$ [Fig. 2(c)] required for our non-volatile CMEs (Figs. 3–5). (Either the calculated value of ε_{cr} has been slightly overestimated due to experimental errors associated with its constituent parameters or the experimental strain has been slightly underestimated due to imperfect strain transfer through the glue affixing the strain gauge.)

The coupling coefficients of our CMEs peak at $\alpha_x = \mu_0 \mathrm{d}M_x/\mathrm{d}E \sim 3.0 \times 10^{-6}$ s m^{-1} [Fig. 3(c)] and $\alpha_y = \mu_0 \mathrm{d}M_y/\mathrm{d}E \sim 8.0 \times 10^{-6}$ s m^{-1} [Fig. 3(d)]. Both of these values exceed the large values achieved using $BaTiO_3$ substrates with epitaxial films of either $La_{0.67}Sr_{0.33}MnO_3$ (2.3×10^{-7} s m^{-1})[16] or FeRh [for which we read 1.4×10^{-6} s m^{-1} from Fig. 3(a), rather than 1.6×10^{-5} s m^{-1} for the virgin effect measured indirectly via temperature sweeps].[31]

In summary, we have exploited uniaxial growth-anisotropy in a CFB film, and anisotropic strain in a PMN-PT $(011)_{pc}$ substrate, to achieve repeatable and non-volatile voltage-driven switching of a large net magnetization at room temperature. In contrast to previously reported CMEs, we did not require the assistance of a magnetic field[26,28] or an in-plane substrate polarization prior to film deposition.[24,25] The CMEs that we report are associated with EA rotations of 90°, and the peak magnetoelectric coupling coefficient of $\sim 8.0 \times 10^{-6}$ s m^{-1} exceeds all previously measured values.[16,31] Miniaturization should lead to single-domain CMEs in which small

Published under license by AIP Publishing

voltages interconvert the values of M_x and M_y in zero magnetic field, resulting in even larger peak coupling coefficients. Taken as a whole, our work represents a step towards the proposed scheme[38,39] of deterministic magnetization reversal via consecutive 90° rotations, and therefore, it represents a step towards future MERAMs.

This work was supported by the National Natural Science Foundation of China (51572123) and the Priority Academic Program Development of Jiangsu Higher Education Institutions (PAPD). D.P. acknowledges Agència de Gestió d'Ajuts Universitaris i de Recerca (AGAUR) from the Catalan government for the Beatriu de Pinós postdoctoral fellowship (2014 BP-A 00079). R.M. acknowledges funding from the Academy of Finland (Grant Nos. 295269 and 306978).

REFERENCES

[1]M. Fiebig, J. Phys. D: Appl. Phys **38**, R123 (2005).
[2]W. Eerenstein, N. D. Mathur, and J. F. Scott, Nature **442**, 759 (2006).
[3]R. Ramesh and N. A. Spaldin, Nat. Mater. **6**, 21 (2007).
[4]G. Catalan and J. F. Scott, Adv. Mater. **21**, 2463 (2009).
[5]M. Bibes and A. Barthélémy, Nat. Mater. **7**, 425 (2008).
[6]J. M. Hu, Z. Li, L. Q. Chen, and C. W. Nan, Nat. Commun. **2**, 553 (2011).
[7]S.-W. Cheong and M. Mostvoy, Nat. Mater. **6**, 13 (2007).
[8]C.-W. Nan, M. I. Bichurin, S. Dong, D. Viehland, and G. Srinivasan, J. Appl. Phys. **103**, 031101 (2008).
[9]H. Ohno, D. Chiba, F. Matsukura, T. Omiya, E. Abe, T. Dietl, Y. Ohno, and K. Ohtani, Nature **408**, 944 (2000).
[10]D. Chiba, M. Yamanouchi, F. Matsukura, and H. Ohno, Science **301**, 943 (2003).
[11]D. Chiba, M. Sawicki, Y. Nishitani, Y. Nakatani, F. Matsukura, and H. Ohno, Nature **455**, 515 (2008).
[12]Y. Yamada, K. Ueno, T. Fukumura, H. T. Yuan, H. Shimotani, Y. Iwasa, L. Gu, S. Tsukimoto, Y. Ikuhara, and M. Kawasaki, Science **332**, 1065 (2011).
[13]T. Maruyama, Y. Shiota, T. Nozaki, K. Ohta, N. Toda, M. Mizuguchi, A. A. Tulapurkar, T. Shinjo, M. Shiraishi, S. Mizukami, Y. Ando, and Y. Suzuki, Nat. Nanotechnol. **4**, 158 (2009).
[14]M. Endo, S. Kanai, S. Ikeda, F. Matsukura, and H. Ohno, Appl. Phys. Lett. **96**, 212503 (2010).
[15]C. Thiele, K. Dörr, O. Bilani, J. Rödel, and L. Schultz, Phys. Rev. B **75**, 054408 (2007).
[16]W. Eerenstein, M. Wiora, J. L. Prieto, J. F. Scott, and N. D. Mathur, Nat. Mater. **6**, 348 (2007).
[17]S. Sahoo, S. Polisetty, C. G. Duan, S. S. Jaswal, E. Y. Tsymbal, and C. Binek, Phys. Rev. B **76**, 092108 (2007).
[18]M. Liu, O. Obi, J. Lou, S. Stoute, Z. Cai, K. Ziemer, and N. X. Sun, J. Phys. D: Appl. Phys. **42**, 045007 (2009).
[19]H. J. A. Molegraaf, J. Hoffman, C. A. F. Vaz, S. Gariglio, D. van der Marel, C. H. Ahn, and J. M. Triscone, Adv. Mater. **21**, 3470 (2009).
[20]T. H. E. Lahtinen, J. O. Tuomi, and S. van Dijken, Adv. Mater. **23**, 3187 (2011).
[21]J. Wang, J. Ma, Z. Li, Y. Shen, Y. H. Lin, and C. W. Nan, J. Appl. Phys. **110**, 043919 (2011).
[22]J. M. Hu, Z. Li, L. Q. Chen, and C. W. Nan, Adv. Mater. **24**, 2869 (2012).
[23]S. Zhang, Q. P. Chen, Y. Liu, A. T. Chen, L. F. Yang, P. S. Li, Z. S. Ming, Y. Yu, W. Sun, X. Z. Zhang, Y. L. Zhao, Y. Sun, and Y. G. Zhao, ACS Appl. Mater. Interfaces **9**, 20637 (2017).
[24]T. Wu, A. Bur, P. Zhao, K. P. Mohanchandra, K. Wong, K. L. Wang, C. S. Lynch, and G. P. Carman, Appl. Phys. Lett. **98**, 012504 (2011).
[25]T. Wu, A. Bur, K. Wong, P. Zhao, C. S. Lynch, P. K. Amiri, K. L. Wang, and G. P. Carman, Appl. Phys. Lett. **98**, 262504 (2011).
[26]S. Zhang, Y. G. Zhao, P. S. Li, J. J. Yang, S. Rizwan, J. X. Zhang, J. Seidel, T. L. Qu, Y. J. Yang, Z. L. Luo, Q. He, T. Zou, Q. P. Chen, J. W. Wang, L. F. Yang, Y. Sun, Y. Z. Wu, X. Xiao, X. F. Jin, J. Huang, C. Gao, X. F. Han, and R. Ramesh, Phys. Rev. Lett. **108**, 137203 (2012).
[27]P. Borisov, A. Hochstrat, X. Chen, W. Kleemann, and C. Binek, Phys. Rev. Lett. **94**, 117203 (2005).
[28]V. Skumryev, V. Laukhin, I. Fina, X. Martí, F. Sánchez, M. Gospodinov, and J. Fontcuberta, Phys. Rev. Lett. **106**, 057206 (2011).
[29]J. T. Heron, J. L. Bosse, Q. He, Y. Gao, M. Trassin, L. Ye, J. D. Clarkson, C. Wang, J. Liu, S. Salahuddin, D. C. Ralph, D. G. Schlom, J. Íñiguez, B. D. Huey, and R. Ramesh, Nature **516**, 370 (2014).
[30]S. Geprägs, A. Brandlmaier, M. Opel, R. Gross, and S. T. B. Goennenwein, Appl. Phys. Lett. **96**, 142509 (2010).
[31]R. O. Cherifi, V. Ivanovskaya, L. C. Phillips, A. Zobelli, I. C. Infante, E. Jacquet, V. Garcia, S. Fusil, P. R. Briddon, N. Guiblin, A. Mougin, A. A. Ünal, F. Kronast, S. Valencia, B. Dkhil, A. Barthélémy, and M. Bibes, Nat. Mater. **13**, 345 (2014).
[32]S. Zhang, Y. Zhao, X. Xiao, Y. Wu, S. Rizwan, L. Yang, P. Li, J. Wang, M. Zhu, H. Zhang, X. Jin, and X. Han, Sci. Rep. **4**, 3727 (2014).
[33]J. J. Yang, Y. G. Zhao, H. F. Tian, L. B. Luo, H. Y. Zhang, Y. J. He, and H. S. Luo, Appl. Phys. Lett. **94**, 212504 (2009).
[34]Y. Chen, T. Fitchorov, Z. Cai, K. S. Ziemer, C. Vittoria, and V. G. Harris, J. Phys. D: Appl. Phys. **43**, 155001 (2010).
[35]M. Ghidini, R. Mansell, F. Maccherozzi, X. Moya, L. C. Phillips, W. Yan, D. Pesquera, C. H. W. Barnes, R. P. Cowburn, J.-M. Hu, S. S. Dhesi, and N. D. Mathur, "Shear-strain mediated magnetoelectric effects revealed by imaging" (unpublished).
[36]D. Hunter, W. Osborn, K. Wang, N. Kazantseva, J. Hattrick-Simpers, R. Suchoski, R. Takahashi, M. L. Young, A. Mehta, L. A. Bendersky, S. E. Lofland, M. Wuttig, and I. Takeuchi, Nat. Commun. **2**, 518 (2011).
[37]Y. T. Chen and C. C. Chang, J. Alloys Compd. **498**, 113 (2010).
[38]Y. Iwasaki, J. Magn. Magn. Mater. **240**, 395 (2002).
[39]R. C. Peng, J. J. Wang, J.-M. Hu, L.-Q. Chen, and C.-W. Nan, Appl. Phys. Lett. **106**, 142901 (2015).